J. Biochem. 119, 487-499 (1996)

Modeling of Continuously and Directly Analyzed Biphasic Reaction Courses of Ribulose 1,5-Bisphosphate Carboxylase/Oxygenase[1]

Akiho Yokota,*,†,[2] Akira Wadano,† and Hiroshi Murayama*,†,[3]

*Plant Molecular Physiology Laboratory, Research Institute of Innovative Technology for the Earth (RITE), Kizu, Kyoto 619-02; and †Department of Agricultural Chemistry, University of Osaka Prefecture, Sakai, Osaka 593

Received for publication, October 9, 1995

This paper aims at clarifying the cause of the time-dependent, partial loss of the activity during reaction (so-called fallover) of ribulose 1,5-bisphosphate carboxylase/oxygenase (RuBisCO) from plant sources. This was done by comparing the reaction courses calculated using the reaction models constructed here based on the present conflicting two ideas on fallover with directly measured courses obtained with RuBisCO purified from spinach leaves. Since the ordinary methods with $^{14}CO_2$ and indicator enzymes were not adequate for analyzing the progress of fallover, we followed the reaction by measuring the change of the light absorbance of ribulose 1,5-bisphosphate (RuBP) at 280 nm. Direct measurements of the reaction course showed that RuBisCO lost its activity with a rate constant of 6.1 to 6.5×10^{-3} s^{-1} at both 0.5 and 2 mM RuBP. The rate constant of the recovery of the enzyme to show the original fallover was determined as 1.2 to 1.3×10^{-3} s^{-1} with RuBisCO that had just experienced fallover. These constants were used in the models. Calculation with a model assuming the binding of xylulose 1,5-bisphosphate (XuBP) to the catalytic sites of the enzyme as the cause of fallover and using the reported dissociation constant of XuBP in the binding and the reported rate of the formation of XuBP from RuBP gave a rather linear reaction course. The minimum requirements for the model to be valid were that the rate of XuBP formation was more than once for every 600 turnovers, the dissociation constant of XuBP for the catalytic sites was less than 0.1 nM, and the binding of XuBP to the sites showed a strong negative cooperativity. Inclusion of non-catalytic RuBP-binding sites in the model was essential to elucidate the course at higher RuBP concentrations. The model constructed assuming that hysteresis was the cause of fallover could calculate the measured reaction courses for the initial 20 min of reaction at both 0.5 and 2 mM RuBP. The rate constants of the hysteretic conformational changes of the predicted enzyme forms to others were given. The direct measurement of the long-term reaction course revealed the two phases in the decay of the activity; fast decay for the initial several minutes and subsequent slow decrease. Although the fast decay could be predicted by the hysteresis model, the slower one required the participation of inhibition by XuBP. We reasoned from these results and the reported characteristics of the binding of other sugar phosphates to the catalytic sites that the initial fast decay of the activity in fallover was due to the hysteretic property of the enzyme and the slower phase of fallover was due to the inhibition by XuBP.

Key words: hysteresis, non-catalytic substrate-binding site (regulatory site), reaction model, ribulose 1,5-bisphosphate carboxylase/oxygenase, xylulose 1,5-bisphosphate.

Ribulose 1,5-bisphosphate carboxylase/oxygenase (RuBisCO) catalyzes the carboxylation and oxygenation reactions of ribulose 1,5-bisphosphate (RuBP). The former reaction forms two molecules of 3-phosphoglycerate (PGA), which is used for synthesis of sugars and for regeneration of RuBP. The oxygenation reaction of RuBP produces 1 mol each of PGA and 2-phosphoglycolate; the latter is dephosphorylated and oxidized to form CO_2 in the glycolate pathway.

RuBisCO requires to be activated by the activator CO_2 and Mg^{2+} to be catalytically competent (*1*). The activation process is comprised of carbamylation of lysine-201 and the subsequent stabilization of the carbamate by the metal ion (*2, 3*). Activated RuBisCO from plant sources shows a gradual decrease in the activity with reaction time to a steady level, as soon as it starts the reaction in the presence of the substrates CO_2 and RuBP (*4-10*). The partial loss of

[1] A part of this work was conducted with the support of the Petroleum Energy Center (PEC) subsidized from the Ministry of International Trade and Industry of Japan.

[2] To whom correspondence should be addressed at: Plant Molecular Physiology, Research Institute of Innovative Technology for the Earth (RITE), 9-2 Kizagawadai, Kizu-cho, Soraku-gun, Kyoto 619-02. Tel: +81-7747-5-2307, Fax: +81-7747-5-2320, e-mail: akiho@rite.or.jp

[3] Present address: Yamasa Shoyu Co., Choshi, Chiba 288.

Abbreviations: 2-CABP, 2-carboxyarabinitol 1,5-bisphosphate; 4-CABP, 4-carboxyarabinitol 1,5-bisphosphate; DTT, dithiothreitol; PGA, 3-phosphoglycerate; RuBP, ribulose 1,5-bisphosphate; RuBisCO, ribulose 1,5-bisphosphate carboxylase/oxygenase; XuBP, xylulose 1,5-bisphosphate.

the activity during the reaction has been called "fallover." Two ideas have been proposed for fallover. One is that inhibitors formed from RuBP on the catalytic sites of RuBisCO through the 2,3-enediol(ate) of RuBP partially inactivate the enzyme (*6, 7, 12-14*). Xylulose 1,5-bisphosphate (XuBP) and 3-ketoarabinitol 1,5-bisphosphate have been identified as the inhibitors (*6, 11, 12, 15*). The former is a much stronger inhibitor of RuBisCO than the latter (*15*). However, there have been no data supporting the occurrence of the complexes between the enzyme and the inhibitors during fallover. The other idea is that the loss of the activity is due to a conformational change of the RuBisCO protein to a low-activity form after the enzyme binds RuBP on the catalytic sites (*9*). This type of change in the activity during enzymatic reaction has been referred to as hysteresis (see Ref. *16* for a review). RuBisCO in the leaves during vigorous photosynthesis appears not to be in the linear phase form, since the activity of freshly extracted RuBisCO shows fallover (*17*). The *in vivo* activity of RuBisCO might be suppressed to some extent by other mechanisms in low light to regulate the balance of the photosynthetic intermediates (*18*). This suggests the possibility that fallover may be regulated in response to irradiance. It would be interesting to know what is the cause of fallover and how this partial decrease of the activity is regulated *in vivo*. To answer these questions on the mechanism of fallover, it is important to construct models based on both ideas and to analyze the reaction courses with the models. This can be accomplished by comparing the constants calculated with the models with those exactly measured and considering the results in relation to evidence from other researches.

In order to examine whether the models based on these ideas can predict the reaction courses measured, reliable measurements are essential. Both ideas, however, have been based upon discontinuous reaction measurements of the carboxylase reaction with $^{14}CO_2$ (*19*). There is a risk in the discontinuous assay that the concentration of volatile $^{14}CO_2$ in the reaction mixture may be changed by repeated withdrawals of aliquots of the mixture. Furthermore, it is impossible to measure the accumulated reaction product as quickly as every 30 s without a large loss of the substrate $^{14}CO_2$. In fact, the observed magnitude of the loss of the activity during fallover varies greatly from laboratory to laboratory (*4, 5, 7, 10*). An often used method to measure the RuBisCO activity continuously is to assay the activity spectrophotometrically using several auxiliary indicator enzymes (*20*). PGA formed in the RuBisCO reaction can be measured with NADH which is oxidized in the conversion of PGA into glycerol 3-phosphate. This method has been used for assaying many enzymes that show a linear time course, with accuracy when the V/K_m value of each indicator enzyme in the mixture exceeds 100 (*21*). This coupling method, however, *per se* may include a lag before reaching a stationary rate, even if the V/K_m value is over 100. Such a lag would be a very serious problem in the assay of an enzyme showing fallover; the extent of fallover may be offset by the lag.

The best way to analyze the biphasic reaction course of an enzyme is to measure directly the concentration of the substrate or the product of the enzyme. Such ketose bisphosphates as RuBP and fructose 1,6-bisphosphate absorb ultraviolet light at around 280 nm (*22*). Rice and Pon (*23*) tried to assay RuBisCO spectrophotometrically by measuring the light absorbance of RuBP at 280 nm. However, the reaction course they obtained was quite far from those generally accepted for plant RuBisCO.

In this study, we devised a reliable method to measure directly the activity of purified RuBisCO. This method was also usable for measuring the activity of the crude extract of spinach leaves. Two models for fallover were constructed to analyze the measured reaction courses. One of them considered the tight binding of XuBP as the cause of fallover and the other was a hysteresis model including inhibition by XuBP. Comparing the reaction courses calculated with the models with the courses followed continuously by the newly devised method has allowed us to resolve the controversy.

MATERIALS AND METHODS

Materials—Spinach RuBisCO was purified as reported previously (*8*) from fresh spinach leaves purchased at the local market. The extract of spinach leaves was also used for the enzyme assay. The cultivation and the preparation of the cell extract of *Escherichia coli* JM109 transformed with pCV23 harboring the genes for both subunits (A and B) of *Chromatium vinosum* (gift from Dr. H. Kobayashi, University of Shizuoka) were done by the methods of Viale *et al.* (*24*). RuBP was synthesized from ribose 5-phosphate using ribose 5-phosphate isomerase and ribulose 5-phosphate kinase by the method of Horecker *et al.* (*25*) and purified by chromatography on Dowex 1-X8, Cl^--form (*26*). Ribose 5-phosphate and these enzymes were obtained from the Sigma Chemical (St. Louis, MO) and ribulose 5-phosphate kinase was desalted with Sephadex G-75 column before use. 2-Carboxyarabinitol 1,5-bisphosphate (2-CABP) was prepared by the method of Pierce *et al.* (*27*).

Assay of RuBisCO—RuBisCO was assayed spectrophotometrically by measuring the decrease of light absorbance of RuBP at 280 nm with a Hitachi U-3210 spectrophotometer. The molecular extinction coefficient of RuBP was low and the oxidation of dithiothreitol (DTT) in the reaction mixture by dissolved oxygen disturbed the measurement at 280 nm. To avoid interference by the DTT oxidation, RuBisCO was assayed in the absence of DTT and oxygen after bubbling all the solutions used in the reaction mixture with N_2 or Ar gas for more than 10 min. RuBisCO was reduced overnight at 25°C with 5 mM DTT in O_2-free 100 mM Hepes/KOH buffer (pH 8.0) containing 1 mM EDTA. DTT was removed from RuBisCO by passing the solution through a column (1 cm × 25 cm) of Sephadex G-25 equilibrated with O_2-free 25 mM Tris/HCl buffer (pH 8.0) containing 1 mM EDTA. RuBisCO was collected in an argon gas-filled small conical vial, and kept in an O_2-free condition at 25°C until use. The stock solutions of $NaHCO_3$ and RuBP were also made O_2-free by dissolving the crystals in O_2-free cold water flushed enough with Ar gas. The reaction mixture before adding $NaHCO_3$, RuBP, and RuBisCO was filtered through a cellulose acetate membrane filter with a pore size of 0.2 μm, and oxygen in the mixture was purged with Ar gas. The O_2-free reaction mixture was put into a 3-ml black quartz cell containing a small stirring bar. The sampling hole of the screw cap of the cell was sealed with thin isoprene rubber and Novix film as reported for a

conical vial for RuBisCO assay (*9*). The temperature of the mixture was maintained at 25°C with a thermoregulator. RuBP and $NaHCO_3$ were added to the mixture, and the carboxylase reaction was started by adding RuBisCO activated in O_2-free 100 mM Hepes/KOH buffer (pH 8.0) containing 1 mM EDTA, 20 mM $MgCl_2$, and 20 mM $NaHCO_3$ for 10 min. Immediately after the additions through the screw cap, the cap was sealed again with Novix film. The consumption of RuBP in the reaction mixture was monitored at 280 nm. The optical density data at this wavelength were stored in a microcomputer and plotted against the reaction time, unless otherwise specified. In the assay of the activity in the crude extract of spinach leaves, RuBisCO was activated and assayed as described above. *Chromatium* RuBisCO synthesized in *E. coli* was assayed by the method of Viale *et al.* (*24*), except that DTT and oxygen were removed from the reaction mixture as above.

To assay RuBisCO with $^{14}CO_2$, $NaH^{14}CO_3$ was substituted for $NaH^{12}CO_3$ in the mixture for the above spectrophotometric assay at the same concentration. After appropriate time intervals, part (50 μl) of the mixture was withdrawn and mixed with 0.2 ml of 4 M formic acid. The acidified mixture was dried at 70°C and acid-stable ^{14}C was counted.

Analysis of the Reverse Reaction of Fallover—The method for preparing DTT-reduced RuBisCO was the same as that described above. RuBisCO was then activated with CO_2 and Mg^{2+} in O_2-free 100 mM Hepes/KOH buffer (pH 8.0) containing 1 mM EDTA, 20 mM $MgCl_2$, and 20 mM $NaHCO_3$ for 10 min. The primary RuBisCO carboxylase reaction was started by adding RuBP to the mixture. The mixture consisted of 100 mM Hepes/KOH buffer (pH 8.0) containing 1 mM EDTA, 20 mM $MgCl_2$, 20 mM $NaHCO_3$, and 0.5 or 2 mM RuBP. The primary reaction proceeded at 25°C for 5 min and was stopped by separating the enzyme from low-molecular-weight compounds using centrifugal gel-filtration of the reaction mixture on Sephadex G-25 at $1,000 \times g$ for 60 s. The eluate was kept in the O_2-free condition until the second reaction was started to see the extent of fallover. The second reaction was initiated by adding the filtered RuBisCO to the new reaction mixture as above. The total time required to start the second reaction was about 2 min after withdrawing the reaction mixture of the first reaction. The initial and steady-state reaction velocities (v_i and v_f, respectively) were calculated by superimposing the measured reaction courses on the theoretical curve for the formation of products in the hysteretic enzyme reaction for time t described as follows (*16*):

$$\text{Products} = v_f \cdot t + [(v_i - v_f)(1 - e^{-k_{obs} \cdot t})]/k_{obs}.$$

k_{obs} is the first-order constant of the decay in the activity calculated by the best-fit analysis of the reaction courses measured at both 0.5 and 2 mM RuBP (for example, see Fig. 6); and the values were 6.1 and 6.5×10^{-3} s^{-1} at 0.5 and 2 mM RuBP, respectively.

MODELING

Since it was unknown whether fallover is caused by inhibitors or by hysteresis at the time of modeling, two models for fallover were constructed based on the two mechanisms.

Inhibitor Model—There is much evidence for the formation of some inhibitors during the carboxylase reaction of RuBisCO (*5, 6, 10-12, 15*). One of the candidates for the cause of fallover in the inhibitor model is XuBP (*6, 12, 15*). We defined XuBP (X) as a representative of known or unknown inhibitors which are responsible for fallover. XuBP is formed from RuBP on the catalytic sites of activated RuBisCO (E) through the 2,3-enediol(ate) of RuBP (*15*). The rate has been calculated as once per 400 to 1,400 turnovers (*7, 10, 15*). The reported dissociation constant of the binding of XuBP to the sites [K_i(X)] is 4 μM (*28*). However, since it is possible that XuBP and/or unknown inhibitors synthesized on the catalytic sites might have much smaller dissociation constants to the sites (T.J. Andrews, personal communication), we took this possibility into account in the modeling. It is known that the recovery of the carboxylase activity is only partial even after the complete removal of the reaction products by gel-filtration (*7, 11*). This has been ascribed to the inhibition of the activity by tight binding of XuBP to the enzyme in the first reaction. On the other hand, fallover was completely reversible when the first reaction time was less than 5 min (see Fig. 4 of the present paper). Taking these results into account, we assumed that the inhibition of the activity of RuBisCO by XuBP proceeded in two steps; reversible binding of XuBP to the catalytic sites to form EX and the subsequent formation of inactive eX after the activator CO_2 had been released (*12, 29*). Formation of EX and eX complexes was regarded as the main cause of fallover in the inhibitor model. Since the rate of the conversion of RuBP into XuBP is very slow in comparison to the rate of RuBP carboxylation in catalysis, XuBP was assumed to be formed not from RuBP on the catalytic sites, but from RuBP in the reaction mixture for simplicity.

The carboxylase reaction consists of the following four steps (*1, 13, 14*); formation of the 2,3-enediol(ate) of RuBP, electrophilic attack at C-2 of the enediol(ate) by the substrate, molecular CO_2, hydration of the formed 2-carboxy-3-ketoarabinitol 1,5-bisphosphate, and cleavage of the carbon bond between C-2 and C-3 to give rise to two molecules of PGA. This complex process was simplified to the following catalytic cycle, including inhibition by XuBP (Scheme 1). Activated enzyme, E, bound RuBP, R, on the catalytic sites and then R reacted with CO_2, C, to form two molecules of PGA, P, which were then released from the enzyme. The carboxylase reaction forms two molecules of PGA from one molecule each of RuBP and CO_2. However, the inhibition of the reaction by PGA has been treated as a simple competitive inhibition with K_i, K_i(P), of 0.84 mM (*30, 31*), and the model assumed the RuBisCO carboxylase reaction to be a two-molecule-forming reaction which was inhibited competitively by one molecule of PGA at the above K_i. The concentration of CO_2 in the reaction mixture was fixed at 0.25 mM, saturating the carboxylase reaction. In the inhibitor model, all of the reactions in the model described above were expressed with differential equa-

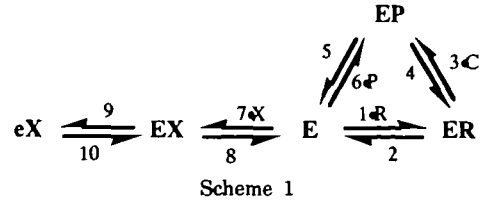

Scheme 1

tions. Through these approximations of the carboxylase reaction, the rate of the consumption of the substrate RuBP, v, which corresponded to half the rate of formation of the product PGA, the rate of the conversion between respective enzyme forms and the rate of the production of XuBP could be expressed as below.

$$v = -dR/dt = dP/2dt = k_5 \cdot [EP] - k_6 \cdot P \cdot [E],$$

$$d[E]/dt = k_2 \cdot [ER] + k_5 \cdot [EP] + k_8 \cdot [EX] - (k_1 \cdot R + k_6 \cdot P + k_7 \cdot X) \cdot [E],$$

$$d[ER]/dt = k_1 \cdot R \cdot [E] + k_4 \cdot [EP] - (k_2 + k_3 \cdot C) \cdot [ER],$$

$$d[EP]/dt = k_3 \cdot C \cdot [ER] + k_6 \cdot P \cdot [E] - (k_4 + k_5) \cdot [EP],$$

$$d[EX]/dt = k_7 \cdot X \cdot [E] + k_{10} \cdot [eX] - (k_8 + k_9) \cdot [EX],$$

$$d[eX]/dt = k_9 \cdot [EX] - k_{10} \cdot [eX],$$

$$d[X]/dt = k_8 \cdot [EX] - k_7 \cdot X \cdot [E] + (k_5 \cdot [EP] - k_6 \cdot P \cdot [E])/400,$$

where $(k_5 \cdot [EP] - k_6 \cdot P \cdot [E])/400$ represents the approximation that XuBP was formed at the rate of once per every 400 RuBP-carboxylations. k_1 to k_6 are the rate constants of the reaction steps in the above scheme, where the subscripts are the numbers of the reaction steps in the model, and were calculated from k_{cat} as below. k_{cat} was determined by best-fit calculation from the measured activity of RuBisCO.

$$k_1 = k_{cat}/K_m(R),\ k_2 = k_1 \cdot K_s(R),\ k_3 = k_{cat}/K_m(C)$$

$$k_4 = k_{cat} \cdot K_i(P)/K_m(C) \cdot K_s(R) \cdot K_e,\ k_5 = k_{cat},\ \text{and}$$

$$k_6 = k_{cat}/K_i(P).$$

$K_m(R)$, Michaelis-Menten constant for RuBP, 20 μM (*32*); $K_m(C)$, Michaelis-Menten constant for CO_2, 10 μM (*32*); $K_s(R)$, dissociation constant of RuBP binding to the catalytic sites, 5 μM (*33*); $K_i(P)$, inhibition constant of PGA, 0.84 mM (*30*); $K_i(X)$, inhibition constant of XuBP added exogenously to the activated enzyme, 4 μM (*28*); K_e, equilibrium constant of the RuBP-carboxylase reaction, 2.979×10^5 (*33*).

Binding of XuBP to the catalytic sites proceeds in a negatively cooperative manner (*12, 28, 29*). In order to take this into account in the model, the dissociation rate of XuBP from EX, k_8, was fixed at 1.2×10^{-3} s^{-1} considering the results of this study (Fig. 4). When $K_i(X)$ was 4 μM, k_7 was estimated as 0.3×10^{-3} s^{-1} μM^{-1}. The active form of RuBisCO in the complex with XuBP, EX, was assumed to change slowly to an inactivated form, eX. Since $K_i(X)$ is 4 μM and the ratio of the concentration of E to that of EX could be calculated as 1 : 2 under their reaction conditions (in the presence of 8 μM XuBP), the rate constant of the formation of eX (k_9) was estimated as 3.75×10^{-3} s^{-1} from the results of McCurry and Tolbert (*28*). The rate constant of the reverse reaction, k_{10}, was expressed as $k_7 \cdot k_9 \cdot K_i'(X)/k_8$, where $K_i'(X)$ is the overall dissociation constant in the formation of eX from E and X. $K_i'(X)$ has been reported to be 0.21 μM (*15*) and k_{10} was calculated as 0.2×10^{-3} s^{-1}. When $K_i(X)$ was varied to estimate the exact $K_i(X)$ for the inhibitor formed on the catalytic sites in the calculation of the reaction course, k_7 was changed based on the equation $K_i(X) = k_8/k_7$, as described in the legends to figures.

Hysteresis-Inhibitor Model—Hysteresis of RuBisCO has been reported (*9*) to be as follows. RuBisCO slowly changes its protein conformation after binding RuBP on the catalytic and non-catalytic sites to other forms with different k_{cat}s depending on the concentration of RuBP in the reaction mixture. Activated RuBisCO (E_1) binds RuBP (R) on the catalytic sites for catalysis to form E_1R when the concentration of RuBP is 0.5 mM or less. RuBP is converted to PGA (P) and E_1 is released. The catalytic cycle composed of the components, E_1, E_1R, and E_1P, was designated as $\langle E_1 \rangle$. E_1R was assumed to be slowly converted to E_2R with 70% less activity. Since the binding of RuBP to the catalytic sites is essential for the conformational change and neither PGA nor XuBP can induce the change (*9*), only E_1R was assumed to be changed to the component, E_2R, of $\langle E_2 \rangle$. When the concentration of RuBP exceeds 0.5 mM, RuBP soon binds to the non-catalytic RuBP-binding sites (*34*). The binding occurs to all components involved in $\langle E_1 \rangle$, and RE_1, RE_1R, and RE_1P in $\langle RE_1 \rangle$ are formed. These three components of RuBisCO change their conformations to the individual stable components in $\langle RE_3 \rangle$. This catalytic cycle has less activity than $\langle E_1 \rangle$ but is more active than $\langle E_2 \rangle$. The superiority of $\langle RE_3 \rangle$ in activity to $\langle E_2 \rangle$ causes an alleviation of the extent of fallover in the presence of more than 0.5 mM RuBP. The $\langle E_2 \rangle$ cycle components also bind RuBP at higher RuBP concentrations to give rise to the $\langle RE_2 \rangle$ components, which then slowly change to the components of $\langle RE_4 \rangle$. The rate of the conversion from $\langle RE_2 \rangle$ to $\langle RE_4 \rangle$ was assumed to be the same as that in the $\langle RE_1 \rangle$ to $\langle RE_3 \rangle$ conversion. However, no change in the activity between $\langle E_2 \rangle$, $\langle RE_2 \rangle$, and $\langle RE_4 \rangle$ has been detected (*9*). The rates of the reverse conversions of $\langle E_2 \rangle$ and $\langle RE_3 \rangle$ to $\langle E_1 \rangle$ were assumed to be 1.15×10^{-3} and 1.33×10^{-3} s^{-1}, respectively, from the results in Fig. 4. All of the rate constants concerning to other conformational changes of the enzyme, which were considered to be very slow in the hysteresis-inhibitor model, were set at one-hundredth of the respective forward reactions (Scheme 2).

The binding of RuBP to the non-catalytic sites was assumed to proceed in a cooperative manner (*9, 34*), where the binding begins as the RuBP concentration exceeds 0.5 mM and is completed at 2 mM. The binding was assumed to proceed with a simple cooperativity (*34*). This could be accomplished by assuming that RuBP bound to the first site with the dissociation constant of 18 mM, then the constant decreased to half of the first constant in the binding to the

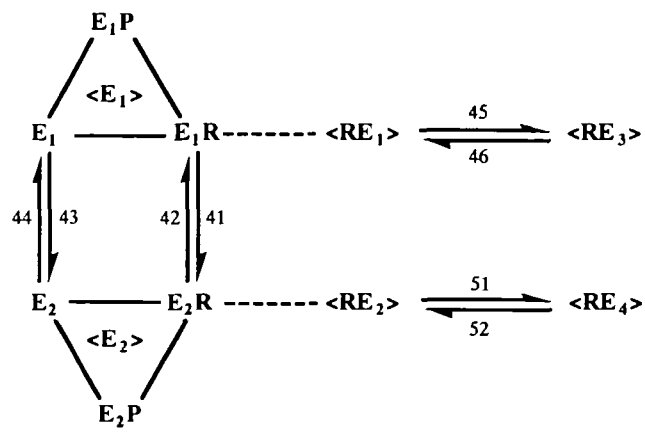

Scheme 2

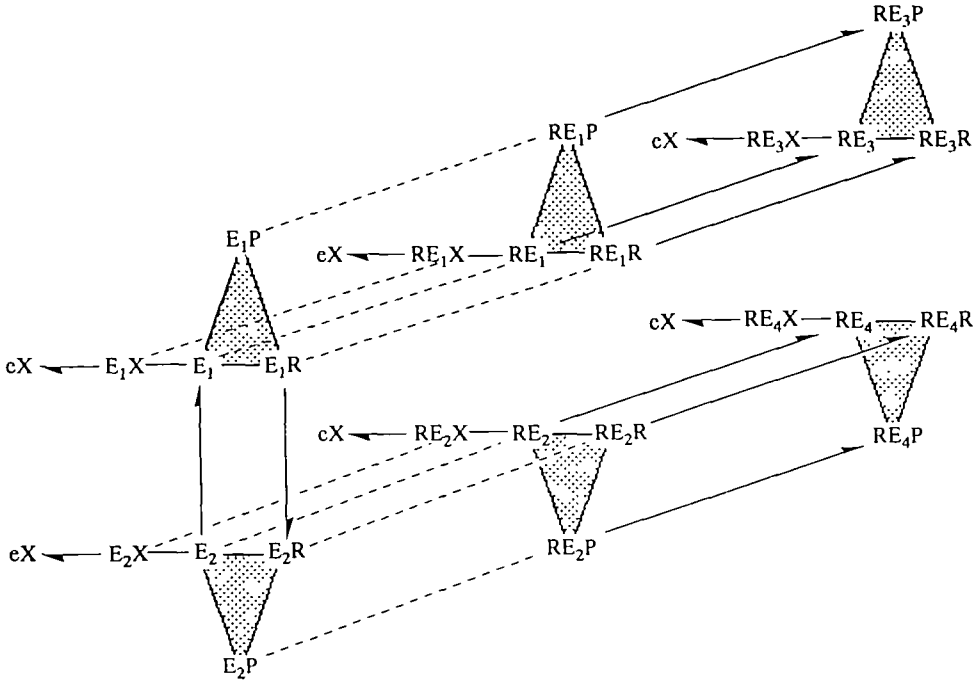

Fig. 1. **Hysteresis-inhibitor model for fallover.** Individual catalytic cycles are depicted with shaded triangles. Each catalytic component in a cycle is connected by a line without an arrowhead. The binding of RuBP to the non-catalytic sites and the subsequent slow change of the protein conformation and the activity are indicated by interrupted lines and solid arrows, respectively. The solid arrows are also the reaction steps, the rate constants of which are matters of interest and calculated by best-fit analysis with a computer.

next site, and so on, until all 8 protomers bound RuBP. Since the rate of the conversion of $\langle RE_1 \rangle$ to $\langle RE_3 \rangle$ is not dependent on the concentration of RuBP (*9*), we assumed that the binding quickly reached equilibrium and then induced another slow change of the protein conformation of RuBisCO. XuBP was assumed to be formed from RuBP at the rate of 1/400 to 1/1,400 of the RuBP-carboxylation rate in the catalytic cycles of any RuBisCO form in Fig. 1. XuBP binds to the catalytic sites of RuBisCO competitively with respect to RuBP (*29*). k_7 was the same as k_1, and k_8 was expressed as $k_7 \cdot K_I(X)$ where $K_I(X)$ was 4 μM. The kinetic constants for the binding of XuBP to the catalytic sites, k_9 and k_{10}, are the same as described in the inhibitor model.

The reaction components (E, ER, EP, and EX) in the individual catalytic cycles were assumed to be in a steady state during the reaction, and the ratio of the amounts of the components was calculated by the King-Altman method. The interconversions of components between the individual catalytic cycles were expressed with differential equations.

Through these approximations of the carboxylase reaction, the rate of the consumption of the substrate RuBP in the $\langle E_1 \rangle$ cycle, v, could be expressed as below.

$$\begin{aligned} v &= -dR/dt = k_1 \cdot R \cdot [E_1] - k_2 \cdot [E_1R] \\ &= \{(k_1 \cdot k_3 \cdot k_5 \cdot k_8 \cdot R \cdot C - k_2 \cdot k_4 \cdot k_6 \cdot k_8 \cdot P) \cdot \langle E_1 \rangle\} / \\ &\quad \{(k_7 \cdot X + k_8)(k_2 \cdot k_5 + k_2 \cdot k_4 + k_3 \cdot k_5 \cdot C) \\ &\quad + k_1 \cdot k_8 \cdot R \cdot (k_3 \cdot C + k_4 + k_5) \\ &\quad + k_6 \cdot k_8 \cdot P \cdot (k_2 + k_3 \cdot C + k_4)\}, \end{aligned}$$

where $\langle E_1 \rangle$ also represents the sum of all enzyme forms in the $\langle E_1 \rangle$ cycle and k_1 to k_8 are the same as those in the inhibitor model. The rate of the consumption of RuBP, or of the carboxylase reaction, in this model is the sum of the reaction velocities of the individual reaction cycles. The rates of the changes in the concentrations of the individual enzyme components (Fig. 1) could be expressed with the following differential equations.

$$\begin{aligned} &d(\langle E_1 \rangle + \langle RE_1 \rangle)/dt \\ &\quad = k_{42} \cdot [E_2R] + k_{44} \cdot [E_2] + k_{46} \cdot \langle RE_3 \rangle \\ &\qquad - (k_{41} \cdot [E_1R] + k_{43} \cdot [E_1] + k_{45} \cdot \langle RE_1 \rangle), \end{aligned}$$

$$\begin{aligned} &d(\langle E_2 \rangle + \langle RE_2 \rangle)/dt \\ &\quad = k_{41} \cdot [E_1R] + k_{43} \cdot [E_1] + k_{52} \cdot \langle RE_4 \rangle \\ &\qquad - (k_{42} \cdot [E_2R] + k_{44} \cdot [E_2] + k_{51} \cdot \langle RE_2 \rangle), \end{aligned}$$

$$d\langle RE_3 \rangle/dt = k_{45} \cdot \langle RE_1 \rangle - k_{46} \cdot \langle RE_3 \rangle,$$

$$d\langle RE_4 \rangle/dt = k_{61} \cdot \langle RE_2 \rangle - k_{62} \cdot \langle RE_4 \rangle, \quad \text{and}$$

$$d\langle eX \rangle/dt = k_9 \cdot [EX] - k_{10} \cdot [eX],$$

where $[EX] = [E_1X] + [RE_1X] + [E_2X] + [RE_2X] + [RE_3] + [RE_4X]$.

The rate constants for the interconversions of the enzyme components and k_{cat} in each reaction cycle were calculated through comparisons between the exactly measured reaction courses and the calculated courses by best-fit analysis with a computer.

RESULTS

Validity of the Spectrophotometric Method for Assay of RuBisCO—Tetrasodium salt of RuBP showed a clear light absorption peak at around 280 nm (Fig. 2). The magnitude of the absorbance and the peak wavelength were not influenced by pH between 7 and 8.5 nor by chelation of the phosphate groups of RuBP by Mg^{2+}, in contrast to fructose 1,6-bisphosphate (*22*). Since there was no light absorbance by PGA around 280 nm, we adopted the molecular extinction coefficient of 50 for RuBP in the RuBisCO assay.

Because of the low extinction coefficient, the spectrophotometric analysis of the RuBisCO reaction course required some important precautions. Sulfhydryl compounds absorb light below 300 nm with an absorption peak around 230 nm at alkaline pHs. Under the slightly alkaline

conditions where RuBisCO is most active, the sulfhydryl group is oxidized by molecular oxygen to give rise to disulfide. The oxidation also causes a decrease of absorbance at 280 nm. In order to avoid this interference, RuBisCO was kept free from O_2 and DTT after reactivation with DTT.

Figure 3A shows an inverted exact trace of the decrease of light absorbance of RuBP at 280 nm in the reaction course of RuBisCO. The inversion of the trace was convenient for visualizing the progress of the reaction. In Fig. 3B, data stored in a microcomputer were plotted to show the change in the RuBP concentration in the reaction mixture (dots), together with the amount of $^{14}CO_2$ fixed in the same reaction mixture (open circles), against reaction time. The change in the RuBP concentration matched well to the amount of $^{14}CO_2$ fixed. The change in absorbance at 280 nm during the reaction could not be ascribed to a change in the protein conformation, since the concentration of RuBisCO in the reaction mixture was too low to allow detection of its absorbance change (*36*). 2-CABP is a structural analogue of a reaction intermediate of RuBisCO and binds to the catalytic sites with a dissociation constant of less than 10 pM to inhibit the catalysis very strongly (*27, 35*). The change in the RuBP concentration measured spectrophotometrically was completely inhibited by a sufficient concentration (100 μM) of 2-CABP (data not shown).

This spectrophotometric method to assay RuBisCO was applicable to a crude extract of spinach leaves. The specific activity of the enzyme in an extract of spinach leaves was 0.3 μmol·mg protein^{-1}·min^{-1} in the initial 1 min burst. This value was quite similar to that measured with $^{14}CO_2$. The whole reaction course of the enzyme in the crude extract was very similar to that with purified enzyme (Fig. 3). While plant RuBisCO shows such a biphasic reaction course as depicted in Fig. 3, the reaction course of RuBisCO from photosynthetic bacteria, cyanobacteria, and green microalgae is linear with reaction time (*8, 37, 38*). This spectrophotometric method also could follow the reaction course of RuBisCO synthesized in *E. coli* transformed with a plasmid carrying the genes for the enzyme of the photosynthetic bacterium, *Chromatium vinosum* (data not shown).

Calculations of the Reaction Courses with Fallover Models—It was required to determine the rate constants of the reverse reactions of fallover to construct the fallover models. This could be done by analyzing the extent of fallover after the start of the reaction of RuBisCO which had just experienced fallover at both 0.5 and 2 mM RuBP and had been freed from the remaining RuBP, free inhibitors, and the reaction product by centrifugal gel-filtration. The plots of the extent of fallover against time after gel-filtration are shown in Fig. 4. Increase of the extent of fallover, or decrease of the ratio of the activity in the final linear phase to the initial activity, v_f/v_i, with time after gel-filtration proceeded in a first-order manner. The value of v_f/v_i just after gel-filtration was about 0.6. The reason why the value was not close to unity (*i.e.*, a linear course) may be that the conformational change of the enzyme or the tight binding of XuBP was not completed for the reaction

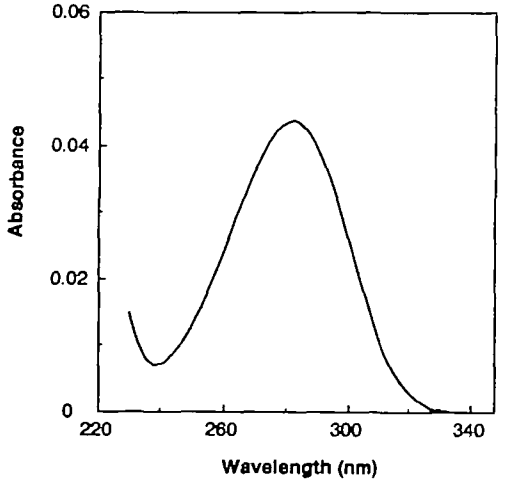

Fig. 2. **Absorption spectrum of RuBP.** Commercial tetrasodium salt of RuBP purified by the method of Pierce *et al.* (*27*) for the purification of 2-CABP was dissolved in 0.1 M Hepes/KOH buffer (pH 8.0) immediately before measurement. The concentration of RuBP was 0.86 mM.

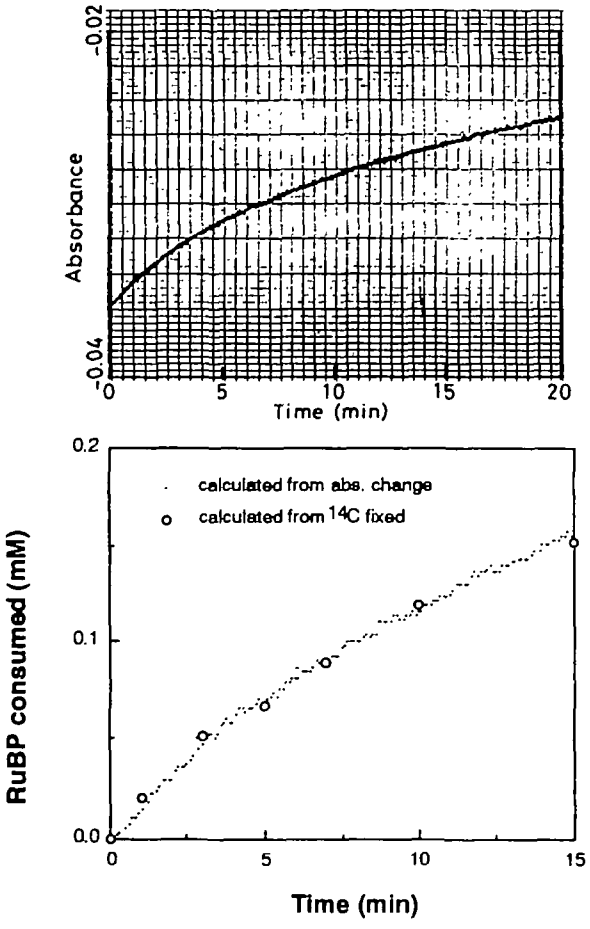

Fig. 3. ***Course of the carboxylase reaction of RuBisCO measured spectrophotometrically.*** The upper panel (A) is the inverted direct trace of the reaction course with 50 μg of RuBisCO. The specific activity in the initial burst was 1.92 μmol·mg protein^{-1} ·min^{-1}. In the lower panel (B), the reaction was followed simultaneously with a spectrophotometer and $^{14}CO_2$ (203 dpm·nmol^{-1}). The RuBisCO concentration was 10 μg per 3 ml of reaction mixture. The specific activity was 1.7 μmol·mg protein^{-1} ·min^{-1} at the initial burst.

time of 5 min and/or that some reverse reaction of fallover proceeded before starting the second reaction. A longer reaction time for the primary reaction was not adequate for this experiment since RuBP in the primary reaction was almost consumed in the reaction time because of the high concentration of the enzyme. Furthermore, it took about 2 min to remove low-molecular-weight compounds by the method employed. After leaving the eluate of gel-filtration of the primary reaction mixture for 60 min, the value of v_f/v_i approached that seen in the reaction course of freshly activated RuBisCO (Fig. 3). This indicates that the enzyme had completely reverted to the original state. The increase in the extent of fallover (decrease of v_f/v_i) corresponds to the backward change of the conformation of the enzyme from $\langle E_2 \rangle$ and $\langle RE_3 \rangle$ into the E_1 form in $\langle E_1 \rangle$ in hysteresis, and the slow release of bound XuBP from the catalytic sites in the inhibitor model. The plot of v_f/v_i against time after gel-filtration was superimposed on the theoretical first-order decay curve to give the rate constant of 1.2×10^{-3} s^{-1}, corresponding to a half time of about 10 min, at 0.5 mM RuBP (Fig. 4A). This value was used in the inhibitor model

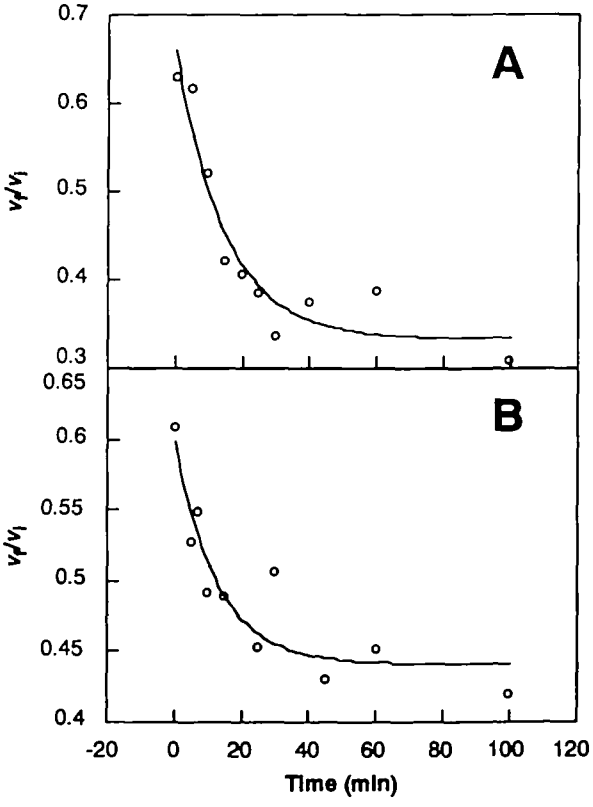

Fig. 4. **Recovery of the biphasic reaction course of RuBisCO which has just experienced fallover at 0.5 (A) and 2.0 mM RuBP (B).** RuBisCO was reacted for 5 min at the protein concentration of 200 μg per 0.5 ml of the primary reaction mixture. The mixture was passed through a column (0.6 cm × 2 cm) of Sephadex G-75 by centrifugation as described in "MATERIALS AND METHODS." The gel had been equilibrated with the same buffer as the primary reaction mixture except that RuBP had not been included and the equilibrating buffer had been removed by centrifugation at 1,000 × g for 1 min just before use. Fifty microliters of the eluate was used for the second reaction. Accordingly, the protein concentration was 10 to 15 μg per 3.0 ml of the reaction mixture. v_f/v_i of the each reaction course was determined as detailed in "MATERIALS AND METHODS."

for the dissociation rate of XuBP from the catalytic sites. The rate constant of the recovery of the extent of fallover at 2 mM RuBP was determined in a similar way to be 1.3×10^{-3} s^{-1} (Fig. 4B).

In Fig. 5, the reaction course followed spectrophotometrically with spinach RuBisCO at 0.5 mM RuBP and those calculated with the inhibitor model are compared. The rate of the formation of XuBP was changed from once for every 400 to 1,400 carboxylase turnovers at the reported $K_i(X)$, 4 μM. With the reported $K_i(X)$ and the uppermost reported rate of XuBP formation, the calculated reaction course was virtually linear with time. If the formation of the inhibitor is the cause of fallover that is accomplished in the first several minutes after the start of the reaction, the following conditions must hold; the inhibitor must be formed at a sufficient rate and the inhibition constant of XuBP to bind the catalytic sites must be sufficiently low to guarantee inhibition in the presence of an excess concentration of RuBP in the first several minutes. The inhibition constant was reduced by increasing the k_7 value in the inhibitor model. For the best fit of the calculation to the measured reaction course for the initial several minutes in Fig. 5, the rate of the XuBP formation must have been more than once for every 600 turnovers and the inhibition constant less than 0.1 nM.

The inhibition of RuBisCO in the absence of RuBP proceeds in a slow, negatively cooperative manner. In Fig. 6, the negatively cooperative property of the inhibition was incorporated in the model. It was assumed in this calculation that the dissociation constant of XuBP was 1 pM and was increased 5.62 times for every binding of XuBP to the catalytic sites and that the rate of the XuBP formation was once for every 400 turnovers. The calculation course fitted well to the measured course at 0.5 mM RuBP. A similar calculation course was obtained with the XuBP formation rate of once for every 600 turnovers. However, increasing the RuBP concentration in the reaction mixture to 2 mM only slightly relieved RuBisCO from the inhibition by XuBP, particularly in the later part of the reaction course, but could not increase the activity to the measured level. This indicates that the simple inhibitor model cannot explain the two types of reaction courses at different RuBP concentrations. This point will be dealt with below.

Figure 7 shows the measured reaction courses of RuBisCO at 0.5 and 2 mM and the courses calculated based on the hysteresis-inhibitor model in Fig. 1 at these RuBP concentrations. In this model, $K_i(X)$ was assumed to be 4 μM, and the rate of the XuBP formation was once for every 1,400 turnovers. The reaction courses measured at 0.5 and 2 mM RuBP could be superimposed by the courses calculated based on the assumptions made in this model. The rate constants in the conversions of the RuBisCO form $\langle E_1R \rangle$ to other forms and the k_{cat} values of the individual reaction cycles were calculated to give the best-fit course at both RuBP concentrations. The calculated k_{cat} of the E_1 cycle (2.1 s^{-1}) decreased to 0.6 s^{-1} in the E_2 cycle during fallover at 0.5 mM RuBP. In the presence of 2 mM RuBP, the activity of the reaction components immediately after binding RuBP at the non-catalytic sites was 24% higher than that in the E_1 cycle and then decreased by 43% during the conformational change in fallover. The rate constants of the conversions of the E_1 cycle to E_2 and E_3 were 0.14 s^{-1} and 2.8×10^{-3} s^{-1}, respectively. Similar results were ob-

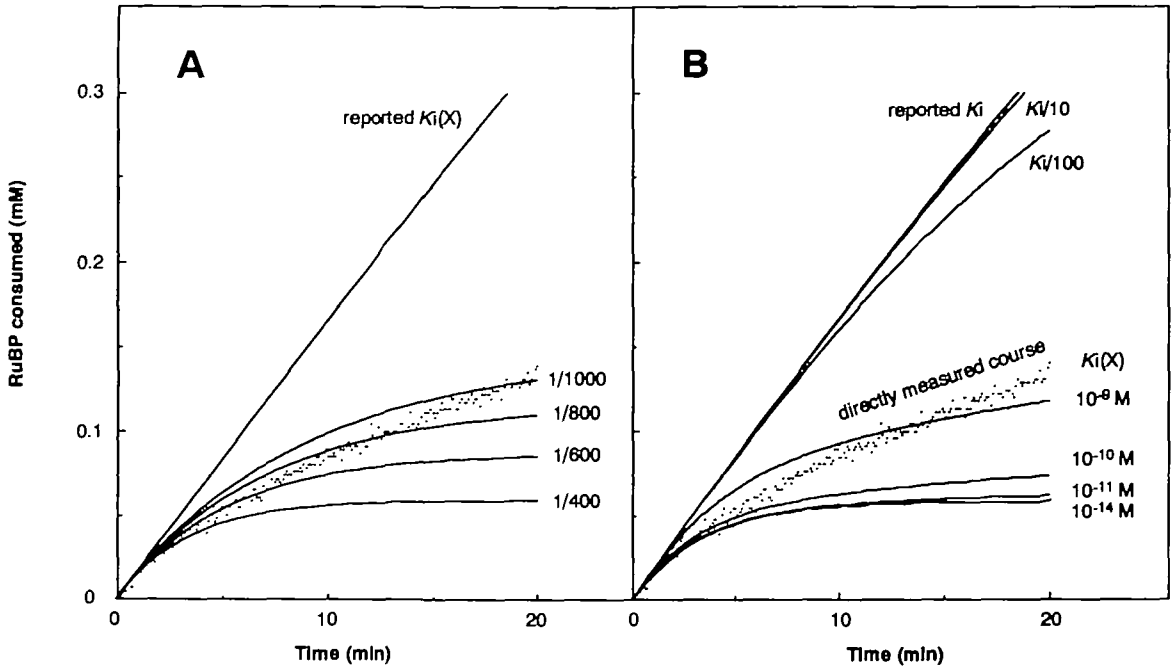

Fig. 5. **Reaction courses of RuBisCO directly measured spectrophotometrically and calculated based on the inhibitor model.** (A) The line designated "reported $K_i(X)$" shows the calculation results obtained assuming that the dissociation constant of activated RuBisCO for XuBP is 4 μM and the rate of the formation of XuBP is once for every 1,400 turnovers. Curvilinear plots are the results on the assumption that the dissociation constant is 10 fM (obtained by increasing k_r to 1.2×10^{11} s^{-1}) and the rate of the formation of XuBP is 1/1,000 to 1/400 of that of the carboxylation reaction. (B) The dissociation constant for XuBP was changed between the reported value (4 μM) and 10 fM. In both panels, RuBisCO was assayed spectrophotometrically with 10 μg of RuBisCO per 3 ml of reaction mixture. The concentration of the catalytic sites corresponded to 48 nM.

tained even if the $K_i(X)$ value was changed between 0.4 and 4 μM.

In Fig. 6, we could not fit the calculated curve to the measured reaction course at 2 mM RuBP in the inhibitor model. Another mechanism for the increment of the activity at the higher concentration of RuBP must be incorporated in the inhibitor model. Then, we assumed that fallover was due to the accumulation of XuBP and the large increase in the activity at 2 mM RuBP was caused by the binding of RuBP to the non-catalytic sites of RuBisCO (Fig. 6). The characteristics of the binding of RuBP to the sites used in this model were the same as those used in the hysteresis-inhibitor model, but hysteretic conformational change of the RuBisCO protein after the binding was not adopted in this case. The calculation curve at 2 mM could be completely superimposed on the measured course. It was found, in this best-fit analysis, that the initial k_{cat} of the reaction cycle of the enzyme carrying RuBP at the non-catalytic sites was 2.6 s^{-1} and that $K_i(X)$ increased from 30 pM to 300 nM in a negatively cooperative manner.

The comparisons of the measured reaction courses and the courses calculated with the models indicate that fallover inherent in plant RuBisCO can be explained by either model. However, this conclusion for the inhibitor model depends upon the following assumptions; namely, (i) $K_i(X)$ is less than 0.1 nM, (ii) the rate of the formation of XuBP is more than once for every 600 turnovers, and (iii) RuBP binds to the non-catalytic sites when its concentration exceeds 0.5 mM.

Long-Term Analysis of Fallover—It has been found that XuBP is simply a competitive inhibitor with respect to RuBP in the presence of RuBP (*29*) but slowly inactivates the enzyme by eliminating an activator CO_2 in the absence of RuBP or during catalysis at lower pHs less than 8.0 (*10, 12*). It would be interesting to investigate the extent of the inhibition of RuBisCO by hysteresis or by XuBP while the concentration of RuBP is decreasing with the progress of the reaction. Similar assay conditions were adopted by Edmondson *et al.* (*4*) for the analysis of fallover. As shown in Fig. 8, we re-examined the reaction course obtained with coupling enzymes by Edmondson *et al.* (see Fig. 4 of Ref. *4*) by our spectrophotometric method, and the reaction course was calculated with the models to examine the contributions of hysteresis and XuBP to the loss of the activity of RuBisCO during its reaction. The reaction was started by adding activated RuBisCO to the reaction mixture containing 0.5 mM RuBP. The reaction course in the primary reaction was composed of three parts; the initial rapid decrease of the activity, the second slower loss, and the final decay due to the consumption of RuBP. RuBP was almost consumed after 80 min. Then, RuBP was further added to the reaction mixture to give a concentration of 0.5 mM to start the second reaction. The activity in the second reaction after the readdition of 0.5 mM RuBP was 80% lower than that in the primary reaction. These reaction courses were calculated with the models and the extents of the contributions of hysteresis and of XuBP and 3-phosphoglycerate to the decreased activity in the second reaction were predicted from the calculation. The reaction course predicted by the hysteresis-inhibitor model using the reported $K_i(X)$ fitted well to the measured course for the initial 20 min but thereafter deviated slightly from the

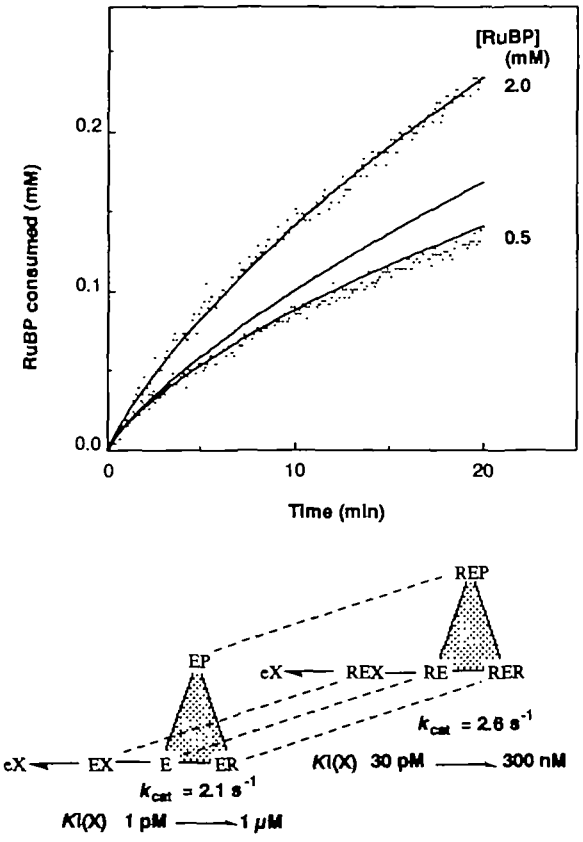

Fig. 6. **Reaction courses calculated based on the inhibitor model on the assumption that binding of XuBP to the catalytic sites proceeds in a negatively cooperative manner.** The reaction courses exactly measured in the presence of 0.5 and 2 mM RuBP at the RuBisCO concentration of 10 μg/3 ml are shown with dotted lines. The dissociation constant in the binding of XuBP to the first site was assumed to be 1 pM with k_7 of 1.2×10^9 s$^{-1}\cdot\mu$M^{-1} at 0.5 mM RuBP, and the rate of increase of the constant was obtained by best-fit analysis. The reaction course at 2.0 mM RuBP was calculated with the modified inhibitor model, where the non-catalytic sites were assumed to be present on the enzyme to increase the k_{cat} value. In this case, the dissociation constant of the first binding and the rate of the increase of the constant were calculated by best-fit analysis. The calculation results are shown under the reaction course panel. The curve which did not fit the measured curve shows the calculated results obtained without incorporating the binding of RuBP to the non-catalytic sites. See the text for details on this point.

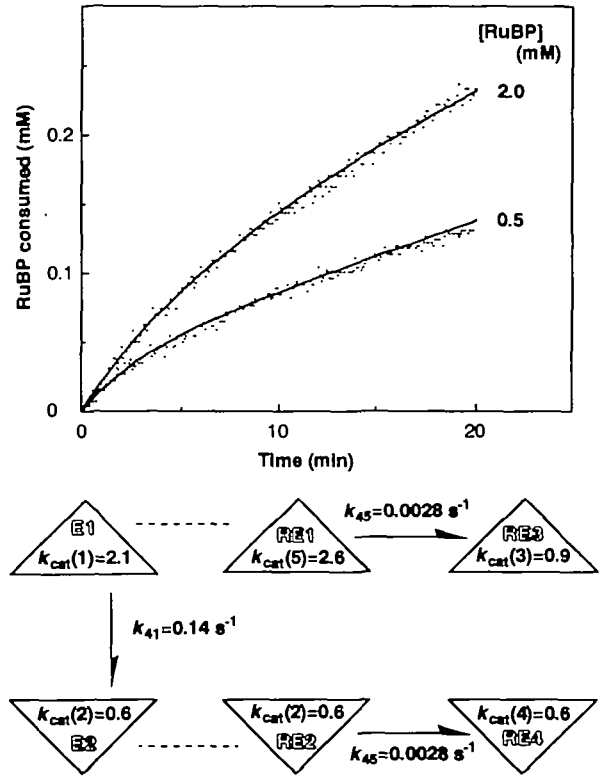

Fig. 7. **Reaction courses calculated based on the hysteresis-inhibitor model at 0.5 and 2 mM RuBP.** The reaction courses exactly measured with 10 μg of RuBisCO in the presence of 0.5 and 2 mM RuBP are shown with dotted lines. The lower panel shows the rate constants of the slow-step reactions depicted by solid arrows in Fig. 1 and the k_{cat} values of the catalytic cycles obtained by best-fit analysis.

measured course. However, reducing K_I(X) to one-tenth of the reported value by increasing k_7 10-fold in the hysteresis-inhibitor model caused this model to calculate these reaction courses nicely. The semi-logarithmic plot of the best-fit curve against the reaction time divided the reaction course much more clearly into three parts (inset of Fig. 8). The rate constant of the decay of the activity was 5×10^{-3} s^{-1} in the initial several minutes and 3×10^{-4} s^{-1} in the second phase in the decrease. The calculation also showed that 60% of the decreased activity in the second reaction was due to the formation of the inactive eX complex of RuBisCO and XuBP and 0.5% by the competition by PGA. The remaining part of the inhibition was due to an accumulation of the low-activity form (E_2) predicted in the hysteresis-inhibitor model (Fig. 1). These percentages are consistent with the conclusions of Robinson and Portis (7) and Edmondson *et al.* (6). The best-fit reaction course could be also obtained with the inhibitor model using the parameters of Fig. 6. In this case, the main cause of the low activity in the second reaction was the formation of the eX form of RuBisCO.

DISCUSSION

In this study, we devised a method to measure the activity of RuBisCO from the decrease in absorbance of RuBP at 280 nm (*23*). The method overcame the disadvantages of the previous assay methods; discontinuity in the assay with $^{14}CO_2$ and unavoidable contamination by the lag in the coupling assay. This direct assay method could follow the decrease of the concentration of RuBP and did not require periodical sampling of the reaction mixture. We could follow the reaction courses of RuBisCOs of spinach and *Chromatium*, irrespective of the existence of fallover and of the purity of the enzyme, by this method.

In this study, we constructed two models for the fallover observed in plant RuBisCO. The dissociation constant of the formation of the EX form and the overall dissociation constant in the formation of eX from carbamylated RuBisCO and XuBP are reportedly 4 and 0.21 μM, respectively (*15, 28*). The calculation with the inhibitor model using these constants gave an almost linear reaction course for the first 20 min (Fig. 5). Decreasing these constants to one-hundredth still caused no significant change in the

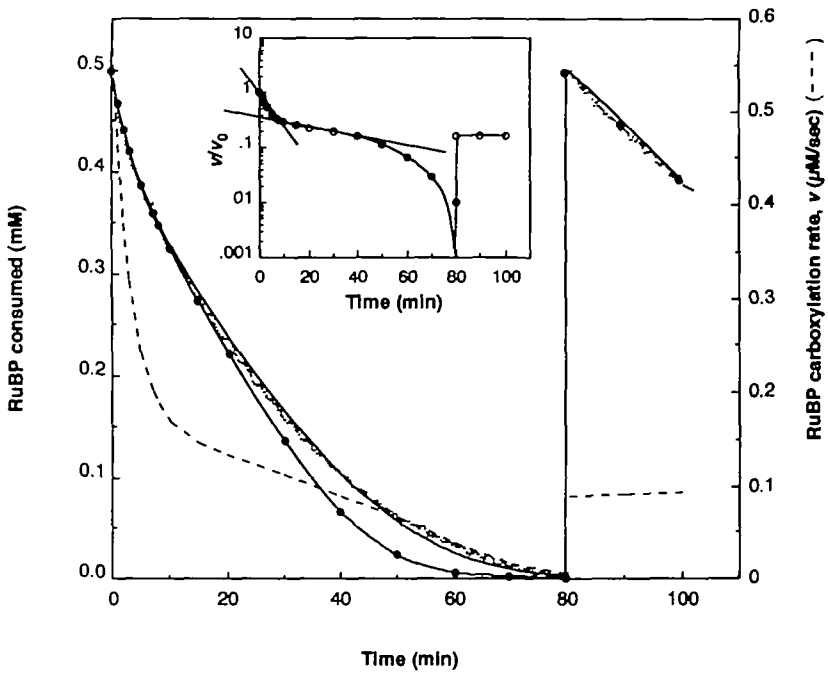

Fig. 8. **Measurement and calculation of the reaction course of RuBisCO in a long-term assay.** The measurement of the reaction was done as in Fig. 3A, except that the concentration of RuBisCO was 30 μg per 3 ml of the reaction mixture. The initial concentration of RuBP was 0.5 mM. At the reaction time of 80 min, a further 0.5 mM RuBP was added. The measured reaction course is shown with dots. The line with closed circles is the reaction course calculated assuming that the hysteresis-inhibitor model used in Fig. 7 is valid. The slight deviation with this model could be minimized by reducing the inhibition constant of XuBP from 4 to 0.27 μM by changing k_7 from 0.3 to 4.4×10^{-3} $s^{-1}\cdot\mu M^{-1}$. The broken line shows the reaction rate at that reaction time calculated from the best-fit curve. The inset is the semilogarithmic plots of the ratios of the activities after various reaction times (v) to that of the initial activity (v_0). The two lines in the inset are regression lines for the initial two components in the decrease in the activity during fallover.

activity for the first 20 min. Since the constants reported previously was not adequate for explaining fallover, there may be a difference in the kinetic constants between XuBP exogenously added to the reaction mixture and that produced on the catalytic site during catalysis (T.J. Andrews, personal communication). It is, however, impossible to know the real reactivity of XuBP or any other inhibitor produced on the catalytic sites in remaining on the sites. Model simulation would be the only way to estimate the extent of inhibition by such inhibitors.

The progress of fallover was not a simple process in which a single inhibition factor was involved. RuBisCO completed the initial rapid decrease in the activity almost 5 min after the start of the reaction (Figs. 3 and 8). The decrease of the activity was completely reversible at this stage, irrespective of the RuBP concentration (Fig. 4). The rates of the recovery from the inhibited states in fallover at both RuBP concentrations in the primary reaction were similar to those in the progress of fallover. The reversible formation of the low-activity form in the initial several minutes can be explained by either the reversible inhibitory binding of XuBP to the catalytic sites of the carbamylated form of the enzyme or the reversible change of the conformation of the enzyme to a low-activity form. Interestingly, RuBisCO that had reacted for a prolonged time was relatively irreversibly inhibited, and RuBisCO remained inhibited strongly even if RuBP was readded to the enzyme which had consumed RuBP in the primary reaction mixture in the prolonged reaction (Fig. 8). The slow, strong inhibition of the activity was not consistent with the idea of hysteresis.

In this study, the possibility of the contribution of some produced inhibitors to fallover was investigated by using a model assuming that inhibition of the activity by the inhibitor is the main cause of fallover. The simulation results suggested that the rate of the formation of the inhibitors should be faster than once for every 600 turnovers and the dissociation constant of the inhibitor should be less than 0.1 nM to follow the reaction course measured directly (Fig. 5). The rate of the production of XuBP was estimated by Andrews *et al.* (*15*) as once per 400 turnovers and this has been generally accepted, although this rate is much faster than those reported by others (*7, 10*). The dissociation constant estimated to validate the inhibitor model, less than 0.1 nM, is close to that of 2-CABP, the transient intermediate analogue that binds almost irreversibly to the sites (K_d of 0.1 to 10 pM) (*27, 35*). In the binding of sugar phosphates to the carbamylated form of RuBisCO, the steric configuration of their carbons is the determinant of the overall dissociation constant of binding (*13, 27, 35, 39*). Of the sugar phosphates examined so far, the strength of the inhibition of RuBisCO is ordered as follows: 2-CABP > 4-carboxyarabinitol 1,5-bisphosphate (4-CABP) > 2-carboxyribitol bisphosphate. The *R*-configuration at carbon 2 is important for sugar phosphates to bind the carbamylated form of RuBisCO *via* three binding sites; two phosphate binding sites (P1 and P2 sites) and Mg^{2+} for the binding of the C-2 carboxyl oxygen (*40*). A large difference of the dissociation constants between 2-CABP and 4-CABP suggests that the configuration at the C-3 carbon is also a determinant of the binding affinity. The fact that 2-CABP has a two-order lower overall dissociation constant for the catalytic sites than 4-CABP (*35*) may suggest that XuBP has a similar order of binding affinity for the sites to RuBP. The present calculation results imply that the inhibition constant of XuBP must have been less than 0.1 nM in the inhibitor model. XuBP is the epimer of RuBP in relation to the C-3 carbon. If the relationship between 2-CABP and 4-CABP resembles that between XuBP and RuBP, the speculated inhibition constant for XuBP may be far from the true value. The hydroxy group on C-3 of XuBP in crystals of the complex between inactivated RuBisCO and XuBP is exactly in the opposite direction to that of the transit analogue 2-CABP (*41*). It is

rather plausible that the inhibition constant of XuBP is near to the dissociation constant of RuBP in the binding to the catalytic sites; as low as 0.01 to 0.1 μM, as predicted in Fig. 7. 3-Ketoarabinitol 1,5-bisphosphate may be another candidate for the cause of fallover. Andrews *et al.* (*15*) have suggested that this sugar phosphate has a larger inhibition constant than XuBP.

The decrease in the activity of RuBisCO in prolonged reaction was composed of three phases; the initial rapid, the second slow, and the final, RuBP concentration-limited parts (Fig. 8). Considering the complete reversibility of the initial rapid decrease in the activity and the inhibition constant of XuBP in its binding to the catalytic sites predicted in this study, this reversible part of fallover should be mainly caused by the hysteretic conformational change of the RuBisCO protein. The second, slower decrease in the activity cannot be explained only by hysteresis. This part in fallover is due to the inhibition by XuBP accumulated during catalysis. The third part of the decrease is due to depletion of the substrate RuBP. Most of the enzyme binds XuBP at this stage and re-addition of RuBP does not cause a recovery of the original activity; RuBisCO showed only 20% of the original activity upon the replenishment of RuBP. Our calculation with the hysteresis-inhibitor model indicated that the strong inhibition was ascribed to three inhibitory components; 60% by XuBP, 0.5% by accumulated 3-phosphoglycerate, and 39% by the retention of the hysteretic low-activity form. The former two components could be removed by gel-filtration or dialysis of the primary reaction mixture, as reported previously (*6, 7*) and deduced from the results in Fig. 4.

The alleviation of the activity in the presence of 2 mM RuBP could not be explained by simple competition of the high concentration of RuBP with XuBP in the inhibitor model (Fig. 6). It was required to incorporate a mechanism that caused the sudden increase in the activity in the presence of the higher concentration of RuBP. We have reported that RuBP binds to the non-catalytic sites in a strongly cooperative manner to increase the activity at more than 1 mM RuBP (*34*). The number of the binding sites is one per enzyme protomer. The exact mechanism of the increase in the turnover rate in catalysis at the catalytic sites by the binding remains to be elucidated. Since RuBisCO changes its protein conformation upon binding (*9*), this change may help the enzyme show a higher turnover rate.

The reaction course predicted from the hysteresis-inhibitor model corresponded well to the measured course both at 0.5 and 2 mM RuBP. On the other hand, the competition of the higher concentration of RuBP for XuBP in the inhibitor model did not have similar effects on the alleviation of fallover as shown in Fig. 6. From these considerations, it was concluded that the time-dependent loss of the activity, inherent in plant RuBisCO, is caused by the hysteretic phenomenon of the enzyme and the alleviation of fallover at higher concentration of RuBP is due to another conformational change of the enzyme caused by the binding of RuBP to the non-catalytic regulatory sites. The inhibition of the activity by XuBP was very significant after the prolonged reaction. It might be concluded that fallover observed for the initial 10 min is due to the hysteretic decrease of the activity and the very slow, continuing loss can be ascribed to the binding of inhibitors at 0.5 and 2 mM RuBP. This

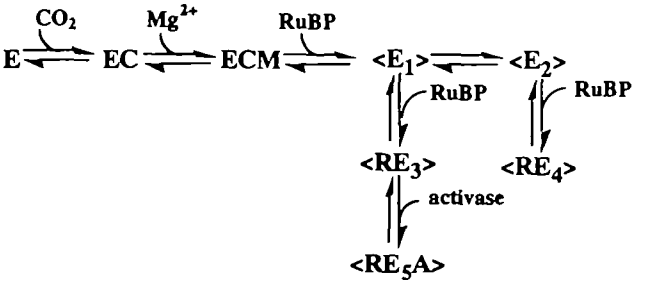

Scheme 3. **Plausible functioning forms appearing in the reaction course of RuBisCO.** The binding of RuBP to the catalytic sites of the ECM form causes the enzyme to function in the E_1 reaction cycle ($\langle E_1 \rangle$). RuBP also binds to the non-catalytic sites to give rise to RE forms. Both A and activase represent RuBisCO activase.

conclusion is consistent with the recent finding by Lee *et al.* (*42*) that the RuBisCO mutant (E48Q) of *Rhorospillirum rubrum* shows strong fallover irrespective of the absence of XuBP.

The severe inhibition of RuBisCO observed as fallover in *in vitro* assay would not take place in *in vivo* conditions, considering the specific activity of RuBisCO observed in the fresh leaves (*43-45*). RuBisCO activase may be important to relieve the enzyme from inhibitors and malfunctions of RuBisCO (*7, 46*). The extinction of fallover by RuBisCO activase had been considered to be due to the removal of the inhibitors from the catalytic sites (*47*). However, since fallover is a consequence of a time-dependent interaction of hysteresis and inhibitors as discussed here, the formation of RuBisCO-RuBisCO activase complex reported by us might be a much more plausible mechanism for the function of RuBisCO activase to keep the enzyme active (*48, 49*). Considering that RuBisCO activase requires the presence of more than 2 mM RuBP, RuBisCO activase would be incorporated in our RuBisCO-functioning model, as shown in Scheme 3. Here, $\langle E_1 \rangle$, $\langle E_2 \rangle$, $\langle RE_3 \rangle$, and $\langle RE_4 \rangle$ are the same as those in the hysteresis-inhibitor model (Fig. 1). Formation of $\langle RE_5\text{-}A \rangle$ by the binding of RuBisCO activase will decrease the equilibrium concentrations of other forms. This scheme is consistent with the reported function of RuBisCO activase, of increasing the affinity of the enzyme for activator CO_2 (*47*). If the activity of $\langle RE_6\text{-}A \rangle$ is no less than that of $\langle E_1 \rangle$, the alleviation of fallover can be explained by this scheme.

We acknowledge helpful discussion with Dr. T.J. Andrews about negative cooperativity in the binding of ligands to RuBisCO and thank Dr. H. Kobayashi, University of Shizuoka, for kindly providing us with *E. coli* transformed with pCV23.

REFERENCES

1. Andrews, T.J. and Lorimer, G.H. (1987) Rubisco: Structure, mechanisms and prospects for improvement in *The Biochemistry of Plants*, Vol. 10 (Hatch, M.D. and Boardman, N.K., eds.) pp. 131-218, Academic Press, New York
2. Lorimer, G.H., Badger, M.R., and Andrews, T.J. (1976) The activation of ribulose-1,5-bisphosphate carboxylase by carbon dioxide and magnesium ions, equilibra, kinetics, a suggested mechanism, and physiological implications. *Biochemistry* **15**, 529-536
3. Lorimer, G.H. (1981) Ribulosebisphosphate carboxylase: Amino acid sequence of a peptide bearing the activator carbon dioxide. *Biochemistry* **20**, 1236-1240

4. Edmondson, D.L., Badger, M.R., and Andrews, T.J. (1990) A kinetic characterization of slow inactivation of ribulosebisphosphate carboxylase during catalysis. *Plant Physiol.* **93**, 1376-1382
5. Edmondson, D.L., Badger, M.R., and Andrews, T.J. (1990) Slow inactivation of ribulosebisphosphate carboxylase during catalysis is not due to decarbamylation of the catalytic site. *Plant Physiol.* **93**, 1383-1389
6. Edmondson, D.L., Badger, M.R., and Andrews, T.J. (1990) Slow inactivation of ribulosebisphosphate carboxylase during catalysis is caused by accumulation of a slow, tight-binding inhibitor at the catalytic site. *Plant Physiol.* **93**, 1390-1397
7. Robinson, S.P. and Portis, A.R., Jr. (1989) Ribulose 1,5-bisphosphate carboxylase/oxygenase activase protein prevents the *in vitro* decline in activity of ribulose-1,5-bisphosphate carboxylase/oxygenase. *Plant Physiol.* **90**, 968-971
8. Yokota, A. and Kitaoka, S. (1989) Linearity and functioning forms in the carboxylase reaction of spinach ribulose 1,5-bisphosphate carboxylase/oxygenase. *Plant Cell Physiol.* **30**, 183-191
9. Yokota, A. (1991) Ribulose bisphosphate-induced, slow conformational changes of spinach ribulose bisphosphate carboxylase cause the two types of inflections in the course of its carboxylase reaction. *J. Biochem.* **110**, 246-252
10. Zhu, G. and Jensen, R.G. (1991) Fallover of ribulose 1,5-bisphosphate carboxylase/oxygenase activity. Decarbamylation of catalytic sites depends on pH. *Plant Physiol.* **97**, 1354-1358
11. Edmondson, D.L., Kane, H.J., and Andrews, T.J. (1990) Substrate isomerization inhibits ribulosebisphosphate carboxylase-oxygenase during catalysis. *FEBS Lett.* **260**, 62-66
12. Zhu, G. and Jensen, R.G. (1991) Xylulose 1,5-bisphosphate synthesized by ribulose 1,5-bisphosphate carboxylase/oxygenase during catalysis binds to decarbamylated enzyme. *Plant Physiol.* **97**, 1348-1353
13. Hartman, F.C. and Harpel, M.R. (1993) Chemical and genetic probes of the active site of D-ribulose-1,5-bisphosphate carboxylase/oxygenase: A retrospective based on the three-dimensional structure. *Adv. Enzymol.* **67**, 1-75
14. Hartman, F.C. and Harpel, M.R. (1994) Structure, function, regulation, and assembly of D-ribulose-1,5-bisphosphate carboxylase/oxygenase. *Annu. Rev. Biochem.* **63**, 197-234
15. Andrews, T.J., Badger, M.R., Edmondson, D.L., Kane, H.J., Morell, M.K., and Paul, K. (1990) Rubisco: Subunits and mechanism in *Current Research in Photosynthesis* (Baltscheffsky, M., ed.) Vol. 3, pp. 331-338, Kluwer, Dordrecht
16. Neet, K.E. and Ainslie, G.R., Jr. (1980) Hysteretic enzymes in *Methods in Enzymology*, Vol. 64 (Purich, D.L., ed.) pp. 192-226, Academic Press, New York
17. Yokota, A., Taira, T., Usuda, H., and Kitaoka, S. (1990) The *in vivo* functioning forms of ribulose 1,5-bisphosphate carboxylase/oxygenase in plants in *Current Research in Photosynthesis* (Baltscheffsky, M., ed.) Vol. 4, pp. 199-202, Kruwer, Dordrecht
18. Mott, K.A., Jensen, R.G., O'Leary, J.W., and Berry, J.A. (1984) Photosynthesis and ribulose 1,5-bisphosphate concentrations in intact leaves of *Xanthium strumarium* L. *Plant Physiol.* **76**, 968-971
19. Lorimer, G.H., Badger, M.R., and Andrews, T.J. (1977) D-Ribulose-1,5-bisphosphate carboxylase-oxygenase: Improved methods for the activation and assay of catalytic activities. *Anal. Biochem.* **78**, 66-75
20. Lilley, R.M. and Walker, D.A. (1974) An improved spectrophotometric assay for ribulosebisphosphate carboxylase. *Biochim. Biophys. Acta* **358**, 226-229
21. Bergmeyer, H.U. (1974) *Methods in Enzymatic Analysis*, 2nd ed., Verlag Chemie, Weinheim
22. McGilvery, R.W. (1965) Fructose 1,6-diphosphate. Acidic dissociation constants, chelation with magnesium, and optical rotatory dispersion. *Biochemistry* **4**, 1924-1930
23. Rice, S.C. and Pon, N.G. (1978) Direct spectrophotometric observation of ribulose-1,5-bisphosphate carboxylase activity. *Anal. Biochem.* **87**, 39-48
24. Viale, A.M., Kobayashi, H., and Akazawa, T. (1990) Distinct properties of *Escherichia coli* products of plant-type ribulose-1,5-bisphosphate carboxylase/oxygenase directed by two sets of genes from the photosynthetic bacterium *Chromatium vinosum*. *J. Biol. Chem.* **265**, 18386-18392
25. Horecker, B.L., Hurwitz, J., and Weissbach, A. (1958) Ribulose diphosphate. *Biochem. Prep.* **6**, 83-90
26. Jordan, D.B. and Ogren, W.L. (1981) A sensitive assay procedure for simultaneous determination of ribulose-1,5-bisphosphate carboxylase and oxygenase activities. *Plant Physiol.* **67**, 237-245
27. Pierce, J., Tolbert, N.E., and Barker, R. (1980) Interaction intermediate partitioning by ribulose-bisphosphate carboxylases with differing substrate specificities. *Biochemistry* **19**, 934-942
28. McCurry, S.D. and Tolbert, N.E. (1977) Inhibition of ribulose-1,5-bisphosphate carboxylase/oxygenase by xylulose 1,5-bisphosphate. *J. Biol. Chem.* **252**, 8344-8346
29. Yokota, A. (1991) Carboxylation and detoxification of xylulose bisphosphate by spinach ribulose bisphosphate carboxylase/oxygenase. *Plant Cell Physiol.* **32**, 755-762
30. Badger, M.R. and Lorimer, G.H. (1981) Interaction of sugar phosphates with the catalytic site of ribulose-1,5-bisphosphate carboxylase. *Biochemistry* **20**, 2219-2225
31. Paulson, J.M. and Lane, M.D. (1966) Spinach ribulose diphosphate carboxylase. I. Purification and properties of the enzyme. *Biochemistry* **5**, 2350-2357
32. Yeoh, H., Badger, M.R., and Watson, L. (1981) Variations in kinetic properties of ribulose-1,5-bisphosphate carboxylases among plants. *Plant Physiol.* **67**, 1151-1155
33. Laisk, A., Eichelmann, H., Oja, V., Eatherall, A., and Walker, D.A. (1989) A mathematical model of the carbon metabolism in photosynthesis. Difficulties in explaining oscillations by fructose 2,6-bisphosphate regulation. *Proc. R. Soc. Lond. B* **237**, 389-415
34. Yokota, A., Higashioka, M., Taira, T., Usuda, H., Wadano, A., and Murayama, H. (1994) Binding of ribulose 1,5-bisphosphate to the non-catalytic sites of ribulose 1,5-bisphosphate carboxylase/oxygenase and its metabolic implications. *Plant Cell Physiol.* **35**, 317-321
35. Schloss, J.V. (1988) Comparative affinities of the epimeric reaction-intermediate analogs 2- and 4-carboxy-D-arabinitol 1,5-bisphosphate for spinach ribulose 1,5-bisphosphate carboxylase. *J. Biol. Chem.* **263**, 4145-4150
36. Jordan, D.B. and Chollet, R. (1983) Inhibition of ribulose bisphosphate carboxylase by substrate ribulose 1,5-bisphosphate. *J. Biol. Chem.* **258**, 13752-13758
37. Andrews, T.J. and Ballment, B. (1984) Active-site carbamate formation and reaction-intermediate analog binding by ribulose-bisphosphate carboxylase/oxygenase in the absence of its small subunits. *Proc. Natl. Acad. Sci. USA* **81**, 3660-3664
38. Yokota, A., Harada, A., and Kitaoka, S. (1989) Characterization of ribulose 1,5-bisphosphate carboxylase/oxygenase from *Euglena gracilis* Z. *J. Biochem.* **105**, 400-405
39. Roach, D.J.W., Gollnick, P.D., and McFadden, B.A. (1983) Interaction of ribulose bisphosphate carboxylase/oxygenase with 2-carboxyhexitol 1,6-bisphosphates. *Arch. Biochem. Biophys.* **222**, 87-94
40. Knight, S., Anderson, I., and Branden, C. (1990) Crystallographic analysis of ribulose 1,5-bisphosphate carboxylase from spinach at 2.5 Å resolution. *J. Mol. Biol.* **215**, 113-160
41. Newman, J. and Gutteridge, S. (1994) Structure of an effector-induced inactivated state of ribulose 1,5-bisphosphate carboxylase/oxygenase: The binary complex between enzyme and xylulose 1,5-bisphosphate. *Structure* **2**, 495-502
42. Lee, E.H., Harpel, M.R., Chen, Y.-R., and Hartman, F.C. (1993) Perturbation of reaction intermediate partitioning by a site-directed mutant of ribulose-bisphosphate carboxylase/oxygenase. *J. Biol. Chem.* **268**, 26583-26591
43. Butz, N.D. and Sharkey, T.D. (1989) Activity ratios of ribulose-1,5-bisphosphate carboxylase accurately reflect carbamylation ratios. *Plant Physiol.* **89**, 735-739
44. Machler, F. and Nosberger, J. (1980) Regulation of ribulose bisphosphate carboxylase activity in intact wheat leaves by light, CO_2, and temperature. *J. Exp. Bot.* **31**, 1485-1491
45. Sage, R.F., Sharkey, T.D., and Seemann, J.R. (1988) The *in vivo* response of the ribulose-1,5-bisphosphate carboxylase activation

state and the pool sizes of photosynthetic metabolites to elevated CO_2 in *Phaseolus vulgaris* L. *Planta* **174**, 407-416
46. Robinson, S.P. and Portis, A.R., Jr. (1988) Release of the nocturnal inhibitor, carboxyarabinitol-1-phosphate, from ribulose bisphosphate carboxylase/oxygenase by rubisco activase. *FEBS Lett.* **233**, 413-416
47. Portis, A.R., Jr. (1992) Regulation of ribulose 1,5-bisphosphate carboxylase/oxygenase activity. *Annu. Rev. Plant Physiol. Plant Mol. Biol.* **43**, 415-437
48. Bruchen-Osmond, C., Portis, A.R., Jr., and Andrews, T.J. (1993) Rubisco activase modifies the appearance of rubisco in the electron microscope in *Research in Photosynthesis* (Murata, N., ed.) Vol. 3, pp. 653-656, Kruwer, Dordrecht
49. Yokota, A. and Tsujimoto, N. (1992) Characterization of ribulose-1,5-bisphosphate carboxylase/oxygenase carrying ribulose 1,5-bisphosphate at its regulatory sites and the mechanism of interaction of this form of the enzyme with ribulose-1,5-bisphosphate carboxylase/oxygenase activase. *Eur. J. Biochem.* **204**, 901-909